Compression of Hyperspectral Images Using Discerete Wavelet Transform and Tucker Decomposition

Mohammad Rami Koujan and Songyou Peng

Supervisor: Prof. Mathini Sellathurai

October 25^{th} 2016

Outline

What is HSI?

Normal image

Combination of only RGB channels, 3 different wavelengths

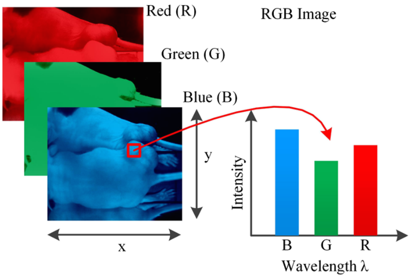

Figure 1: Normal RGB image[1]

[1] Image Courtesy of Lu, Guolan, and Baowei Fei. "Medical hyperspectral imaging: a review." Journal of biomedical optics 19.1 (2014): 010901-010901.

What is HSI?

Hyperspectral image (HSI)

One image usually covers several hundred bands (remote sensing)

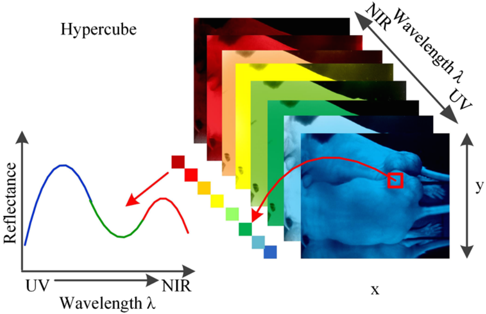

Figure 2: HSI example [2]

[2] Image Courtesy of Lu, Guolan, and Baowei Fei. "Medical hyperspectral imaging: a review." Journal of biomedical optics 19.1 (2014): 010901-010901.

What is HSI?

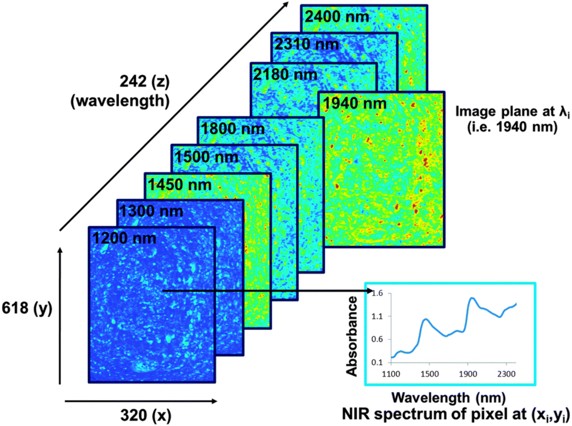

Figure 3: HSI real example in NIR [3]

[3] Image Courtesy of Manley, Marena. "Near-infrared spectroscopy and hyperspectral imaging: non-destructive analysis of biological materials." Chemical Society Reviews 43.24 (2014): 8200-8214.

Why need compression in HSI?

HSI size

HSIs usually have really large size, e.g. $500 \times 500 \times 250$

Redundant information

- Spatial correlation
- Spectral correlation

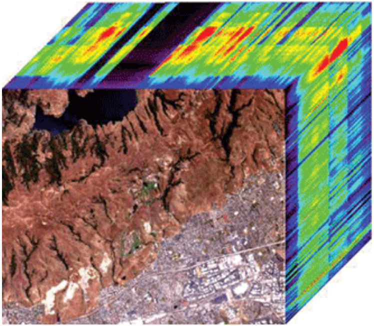

Figure 4: A HSI acquired by Airborne Visible-Infrared Imaging Spectrometer developed by NASA

Workflow

Proposed Algorithm (DWT-TD)

Input: Original HSIs $\underline{\mathbf{X}}$ (the size is $I_1 \times I_2 \times I_3$)

1-Apply 2DWT to each spectral band to obtain 4 sub-images (approximate, diagonal, vertical and horizontal tensors).

2-Apply TD algorithm to the four tensors individually. Each tensor $\underline{\mathbf{Y}}$ has the size of $(I_1/2) \times (I_2/2) \times I_3$

Begin TD

$1 \leq J_1 \leq (I_1/2), 1 \leq J_2 \leq (I_2/2), 1 \leq J_3 \leq (I_3/2)$

Initialize Nonnegative ALS for all $\mathbf{A}^{(n)}$ and $\underline{\mathbf{G}}$

Normalize all $a_{j_n}^{(n)}$ (for $n = 1, \ldots, 3$) to unit length

$\underline{\mathbf{E}} = \underline{\mathbf{Y}} - \hat{\underline{\mathbf{Y}}}$

repeat

for $n = 1$ to 3 do

for $j_n = 1$ to J_n do

$\mathbf{Y}_{(n)}^{(j_n)} = \mathbf{E}_{(n)} + a_{j_n}^{(n)}[\mathbf{G}_{(n)}]_{j_n} A^{\otimes_{-n}T}$

$a_{jn}^{(n)} \leftarrow [\mathbf{Y}_{(n)}^{(j_n)}[(\underline{\mathbf{G}} \times_{-n} \{\mathbf{A}\})_{(n)}]_{j_n}^T]_+$

$a_{j_n}^{(n)} \leftarrow a_{j_n}^{(n)} / \|a_{j_n}^{(n)}\|_2$

$\mathbf{E}_{(n)} \leftarrow \mathbf{Y}_{(n)}^{(j_n)} - a_{j_n}^{(n)}[\mathbf{G}_{(n)}]_{j_n} A^{\otimes_{-n}T}$

end

end

for each $j_1 = 1, \ldots, J_1$, $j_2 = 1, \ldots, J_2$, $j_3 = 1, \ldots, J_3$

$g_{j_1 j_2 j_3} \leftarrow g_{j_1 j_2 j_3} + \underline{\mathbf{E}} \overline{\times} a_{j_1}^{(1)} \overline{\times} a_{j_2}^{(2)} \overline{\times} a_{j_3}^{(3)}$

$\underline{\mathbf{E}} \leftarrow \underline{\mathbf{E}} + \Delta_{g_{j_1 j_2 j_3}} a_{j_1}^{(1)} \circ a_{j_2}^{(2)} \circ a_{j_3}^{(3)}$

end

until *a stopping criterion is met*

Output: 3 factors $\mathbf{A}^{(n)} \in \mathbf{R}^{I_n \times J_n}$ and a core tensor $\underline{\mathbf{G}} \in \mathbf{R}^{J_1 \times J_2 \times J_3}$

End TD

4-Quantize $\mathbf{A}^{(n)} \in \mathbf{R}^{I_n \times J_n}$ and encode core tensor $\underline{\mathbf{G}} \in \mathbf{R}^{J_1 \times J_2 \times J_3}$ Using AAC

Workflow

posed Algorithm (DWT-TD)

Inpu inal HSIs $\underline{\mathbf{X}}$ (the size is $I_1 \times I_2 \times I_3$)

1-Apply 2D o each spectral band to obtain 4 sub-images (approximate, dia l, vertical and horizontal tensors).

2-Apply TD algorithm to r tensors individually. Each tensor $\underline{\mathbf{Y}}$ has the size of $(I_1/2)$) $\times I_3$

Begin TD

$1 \leq J_1 \leq (I_1/2), 1 \leq J_2 \leq (I_2/2), 1 \leq J_3 \leq (I_3/2$

Initialize Nonnegative ALS for all $\mathbf{A}^{(n)}$ and $\underline{\mathbf{G}}$

Normalize all $a_{j_n}^{(n)}$ (for $n = 1, \ldots, 3$) to unit

$\underline{\mathbf{E}} = \underline{\mathbf{Y}} - \hat{\underline{\mathbf{Y}}}$

repeat

for $n = 1$ to 3

$= 1$ to J_n **do**

$\mathbf{Y}_{(n)}^{(j_n)}$ $+ a_{j_n}^{(n)} [\mathbf{G}_{(n)}]_{j_n} A^{\otimes_{-n}T}$

$a_{jn}^{(n}$ $[\mathbf{Y}_{(n)}^{(j_n)} [(\underline{\mathbf{G}} \times_{-n} \{\mathbf{A}\})_{(n)}]_{j_n}^{T}]_{+}$

$a_{j_n}^{(n)} \leftarrow a_{j_n}^{(n)} / \|a_{j_n}^{(n)}\|_2$

$\mathbf{E}_{(n)} \leftarrow \mathbf{Y}_{(n)}^{(j_n)} - a_{j_n}^{(n)} [\mathbf{G}_{(n)}]_{j_n} A^{\otimes_{-n}T}$

end

end

f ch $j_1 = 1, \ldots, J_1$, $j_2 = 1, \ldots, J_2$, $j_3 = 1, \ldots, J_3$

$g_{j_1 j_2 j_3} \leftarrow g_{j_1 j_2 j_3} + \underline{\mathbf{E}} \overline{\times} a_{j_1}^{(1)} \overline{\times} a_{j_2}^{(2)} \overline{\times} a_{j_3}^{(3)}$

$\underline{\mathbf{E}} \leftarrow \underline{\mathbf{E}} + \Delta_{g_{j_1 j_2 j_3}} a_{j_1}^{(1)} \circ a_{j_2}^{(2)} \circ a_{j_3}^{(3)}$

until *a stoppi rion is met*

Output: 3 factors $\mathbf{A}^{(n)} \in \mathbf{R}$ nd a core tensor $\underline{\mathbf{G}} \in \mathbf{R}^{J_1 \times J_2 \times J_3}$

End TD

4-Quantize $\mathbf{A}^{(n)} \in \mathbf{R}^{I_n \times J_n}$ and encode core tensor $\underline{\mathbf{G}} \in \mathbf{R}^{J_1 \times J_2 \times J_3}$ Using AAC

Workflow

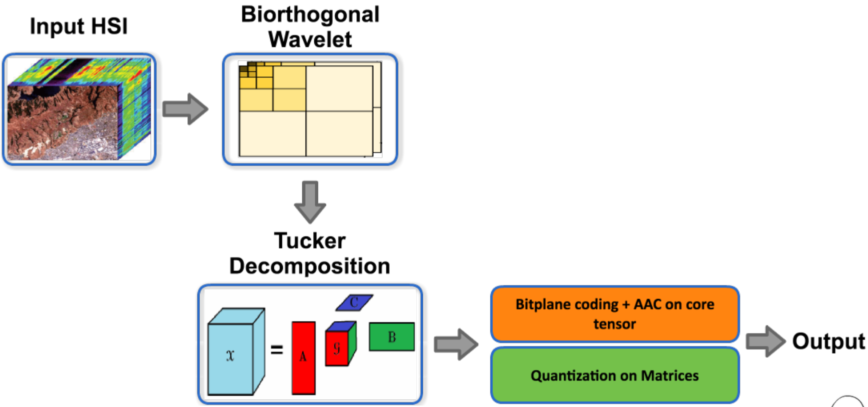
Input HSI
Biorthogonal Wavelet
Tucker Decomposition
$\mathcal{X}$ = A $\mathcal{G}$ B C
Bitplane coding + AAC on core tensor
Quantization on Matrices
Output

Biorthogonal 9/7 Wavelet

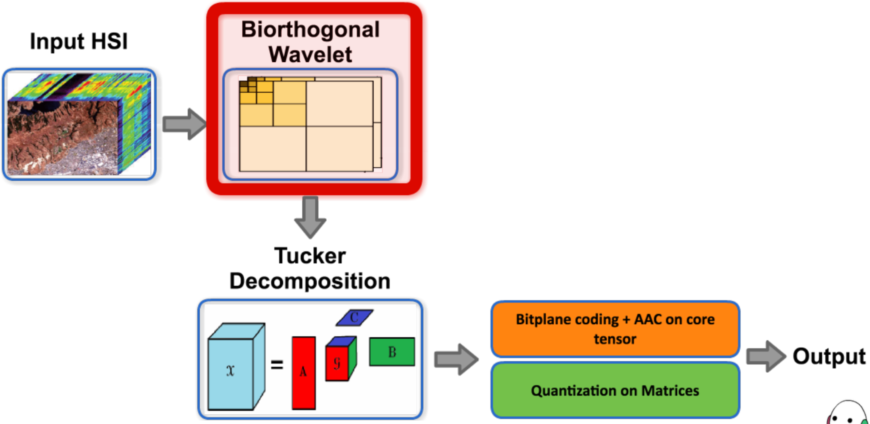

Biorthogonal 9/7 Wavelet

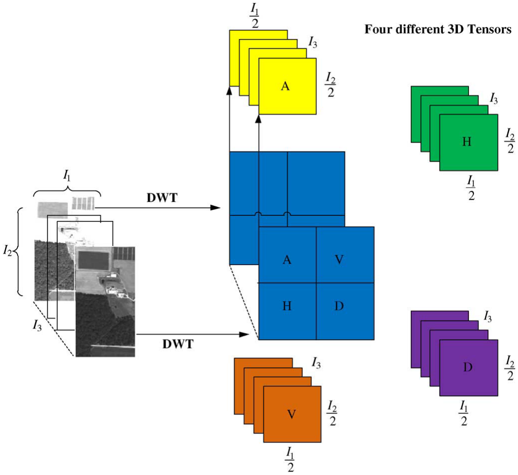

Figure 5: Applying Biorthogonal wavelet to HSIs

Tucker Decomposition

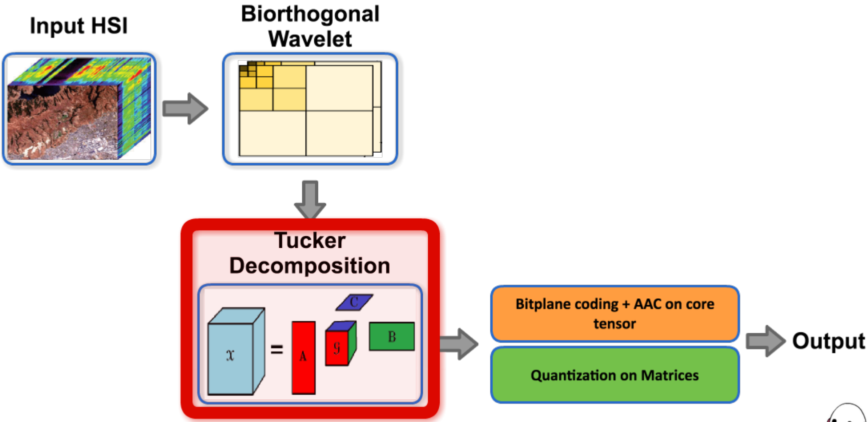

Tucker Decomposition

What is mode-n tensor-matrix product?[4]

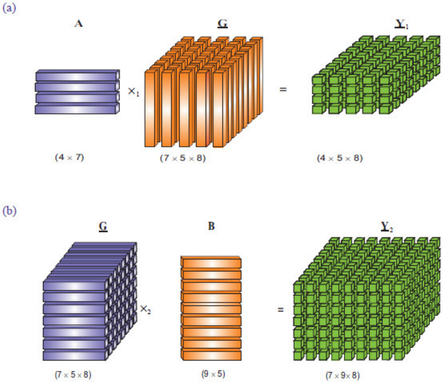

Figure 6: Illustration of the mode-n multiplications of a third-order tensor by matrices. (a) mode-1 multiplication $Y_1 = G \times_1 A$, (b) mode-2 multiplication $Y_2 = G \times_2 B$

[4] Image Courtesy of Cichocki, Andrzej, et al. Nonnegative matrix and tensor factorizations: applications to exploratory multi-way data analysis and blind source separation. John Wiley & Sons, 2009.

Tucker Decomposition

What is mode-n tensor-matrix product?[5]

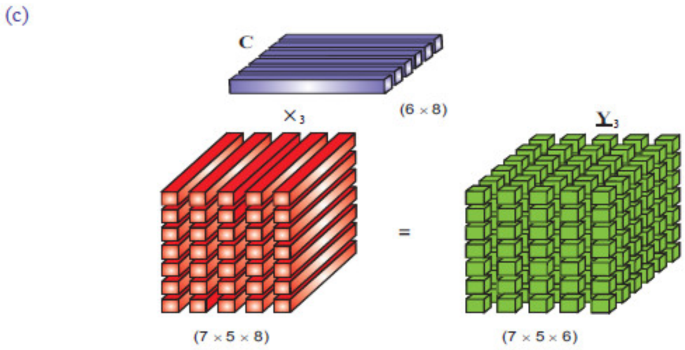

Figure 7: Illustration of the mode-n multiplications of a third-order tensor by matrices. (c) mode- 3 multiplication $Y_3 = G \times_3 C$

[5] Image Courtesy of Cichocki, Andrzej, et al. Nonnegative matrix and tensor factorizations: applications to exploratory multi-way data analysis and blind source separation. John Wiley & Sons, 2009.

Tucker Decomposition

De-correlation in both spatial and spectral domains

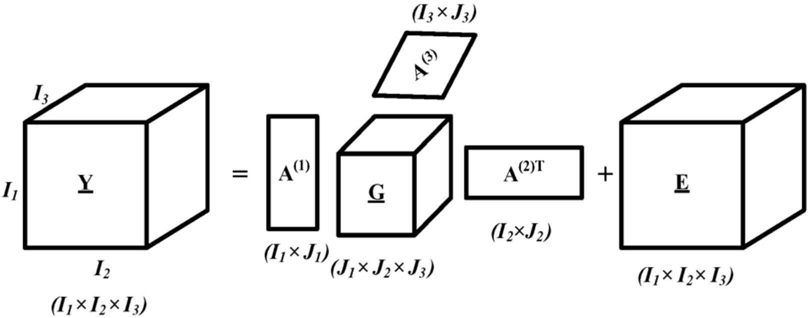

$$\mathbf{D_F}(Y|G, A) = \frac{1}{2}||Y - \hat{Y}||^2 \tag{1}$$

Find optimal component matrices $A^{(n)}$ and core tensor G

Bitplane coding

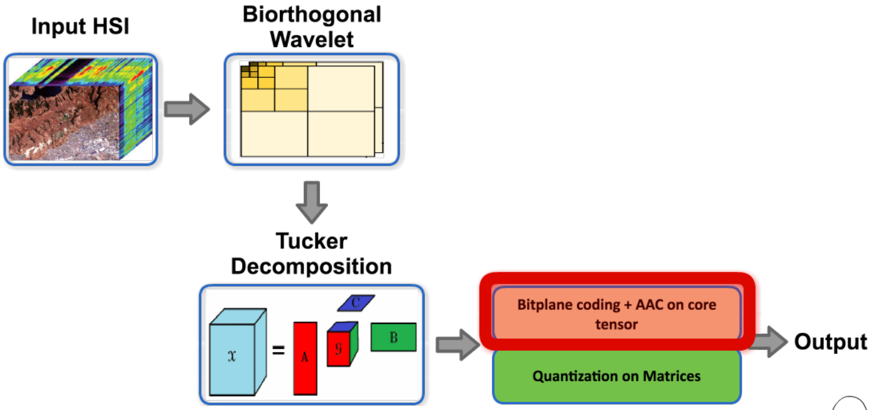

Bitplane coding

Purpose

Reduce the amount of redundant information in the core tensor G

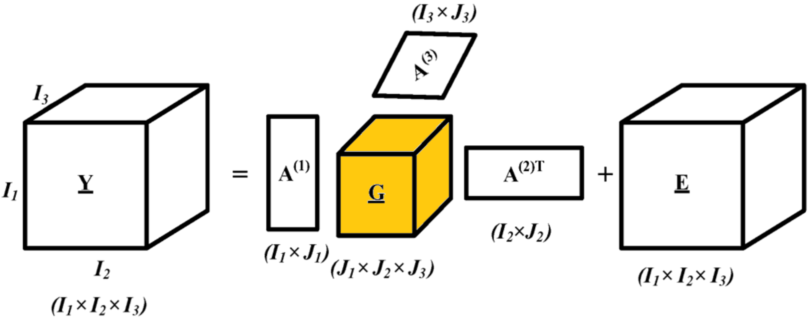

Bitplane coding

How?

Define a significant map with threshold T, state $s_{j_1 j_2 j_3}$, and elements $g_{j_1 j_2 j_3}$ in G

$$s_{j_1 j_2 j_3} = \begin{cases} 1, & T \leq |g_{j_1 j_2 j_3}| \leq 2T \\ 0, & \text{otherwise} \end{cases} \tag{2}$$

Procedure

- If the state $s_{j_1 j_2 j_3} = 1$, $g_{j_1 j_2 j_3}$ is deemed significant, removed from G, and encoded via Adaptive Arithmetic coding (AAC)
- The process is repeated with halved threshold till the energy of the encoded elements equal to 99.5% of core tensor G

Quantization of $A^{(n)}$

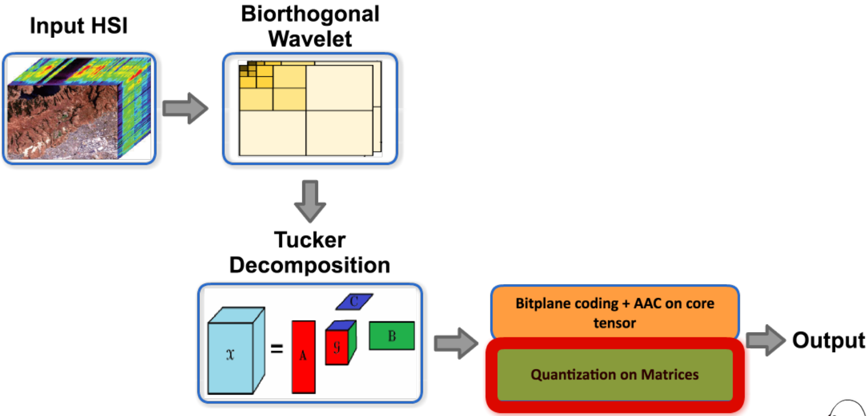

Quantization of $A^{(n)}$

Uniform quantization of $A^{(n)}$

The absolute values of the columns of $A^{(n)}$ have been normalized to the range $[0, 1]$, so they are close to each other.

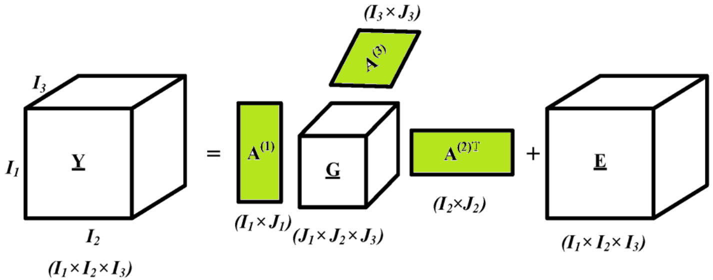

Figure 8: Qunatization of $A^{(n)}$

Quantitative results – SNR

Comparisons in both AVIRIS datasets

DWT-TD significantly improves SNR especially at high compression ratios (small bpppbs)

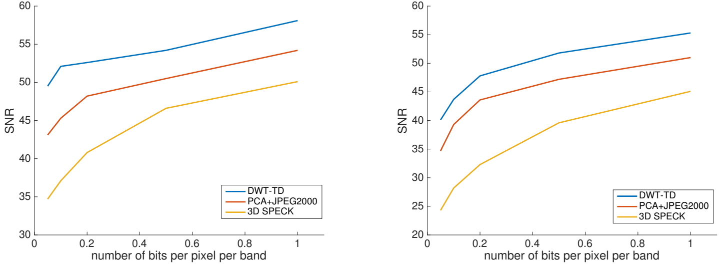

(a) Cuprite (b) Moffett Field

Figure 9: SNR values for DWT-TD, PCA+JPEG2000 and 3D SPECK

Quantitative results – Classification accuracy

Details about the carried-out test

- Tests are performed on the dataset of Indiana's Indian Pine[a]
- Pixel-based SVM is used to classify images
- Lossy compression can cause the local smoothing in the spatial and spectral domain

[a] http://dynamo.ecn.purdue.edu/~biehl/

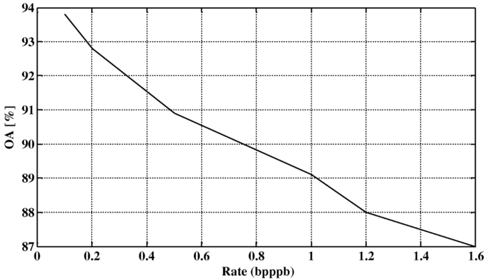

Unmixing results

HSI pixel mixing problem

Many HSIs in remote sensing have low resolution ($> 5m$ per pixel), causing each pixel to be a mixture of several materials.

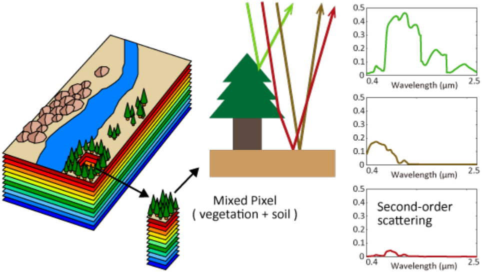

Figure 10: Illustration for HSI unmixing problem[6]

[6] N. Yokoya, J. Chanussot, and A. Iwasaki, " Nonlinear unmixing of hyperspectral data using semi-nonnegative matrix factorization ," IEEE Trans. Geosci. Remote Sens., vol. 52, no. 2, pp. 1430-1437, 2014.

Unmixing results

Unmixing goal

Acquire low spectral angle distance of various materials between compressed and original hyperspectral images.

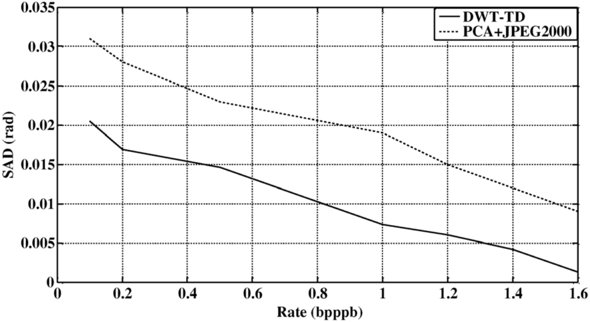

Figure 11: Comparison of unmixing accuracy

Conclusions

DWT – TD compression algorithm for HSI

- Drastically reduce spatial and spectral correlations of HSI
- Achieve higher SNR compared with state-of-the-art methods
- Accomplish better classification accuracy

References

- Karami, Azam, Mehran Yazdi, and Gregoire Mercier. "Compression of hyperspectral images using discerete wavelet transform and tucker decomposition." IEEE journal of selected topics in applied earth observations and remote sensing 5.2 (2012): 444-450.
- Nascimento, Jose MP, and Jose MB Dias. "Vertex component analysis: A fast algorithm to unmix hyperspectral data." IEEE transactions on Geoscience and Remote Sensing 43.4 (2005): 898-910.
- Faloutsos, Christos. "Mining Large Time-Evolving Data Using Matrix And Tensor Tools SIGMOD07". `http://www.cs.cmu.edu/~christos/TALKS/SIGMOD-07-tutorial/` N.p., 2016. Web. 24 Oct. 2016.
- Cichocki, Andrzej, et al. Nonnegative matrix and tensor factorizations: applications to exploratory multi-way data analysis and blind source separation. John Wiley & Sons, 2009.

Compression of Hyperspectral Images Using Discerete Wavelet Transform and Tucker Decomposition

Mohammad Rami Koujan and Songyou Peng

Supervisor: Prof. Mathini Sellathurai

October 25^{th} 2016